

Optical Polarization Driven Giant Relief Modulation in Amorphous Chalcogenide Glasses

K. E. Asatryan, T. Galstian,* and R. Vallée

Centre for Optics, Photonics and Lasers, Laval University, Quebec, Canada G1K 7P4

(Received 22 September 2004; published 2 March 2005)

We report on the observation of giant relief modulation in amorphous chalcogenide As_2S_3 glass under polarization modulated near band gap light illumination. We show that these periodic modulations are created as a result of the photoinduced mass transport despite the very low and uniform intensity light illumination. A phenomenological model, based on a photoinduced alignment of anisotropic microvolumes within the glass, is proposed to explain the phenomenon.

DOI: 10.1103/PhysRevLett.94.087401

PACS numbers: 78.66.Jg, 42.40.Eq, 83.50.-v

In spite of the wide variety of applications currently mastered using amorphous materials, this state of matter still represents a complex system hiding many surprising properties. Among them, amorphous chalcogenide glasses (ChGs) have attracted a great deal of interest thanks to their rich photochemical behavior [1]. However, many intriguing phenomena in these glasses are not well understood at the microscopic level. For example, there is still a wide divergence of opinions concerning the nature of their sensitivity to the intensity and polarization of light. An exciting manifestation of such sensitivity was reported recently by Gump *et al.* [2]. In this work the near band gap light was shown to induce a strong athermal giant softening of the Ge-Se chalcogenide glass network over a narrow compositional range. The understanding of the microscopic mechanisms that are at the origin of the optical properties of chalcogenide glasses thus represents an important scientific and technological challenge.

The observation of weak relief grating (RG) formation in these materials using intensity modulated interference patterns of light with near band gap wavelength is well known and was reported in [3–5]. Recently Saliminia *et al.* reported the observation of strong photoinduced relief modulations in ChG thin films with two tightly focalized ($\sim 100 \text{ W/cm}^2$) laser beams [6]. The strongest relief modulations in this work were observed when the film was exposed by an intensity modulation pattern. A mass transport due to electric field gradient force was suggested to be at the origin of the observed phenomenon. In fact, several mechanisms can be involved in RG formation in such a high intensity recording regime, which complicates the interpretation of experimental results. Note that, from a practical viewpoint, polarization modulation configurations are unavoidably accompanied by weak intensity modulations, except in the case where *s* and *p* polarized laser beams are used for exposure [7]. Note also that in those cases the scalar effects can play a predominant role if the samples are not photodarkened prior to their exposure to the polarization modulated light. Therefore it is difficult to “isolate” and confirm that the mechanism of relief modulations, in the case when spatially modulated polarization is used for exposure, is pure polarization driven.

In this work we present the observation of giant RG formation on photodarkened ChG films occurring for a vector holographic exposure (i.e., uniform intensity) configuration (see, e.g., [8] for vector holography) at very low intensity, i.e., $\sim 100 \text{ mW/cm}^2$, which is 3 orders of magnitude smaller than in the case reported in [6]. We present a phenomenological model that provides a rather good description of the observed phenomenon. Any complete model describing the RG formation must encompass both the driving mechanism responsible for the internal force gradient and the RG buildup process itself, i.e., the nature of the material deformation resulting from the application of this internal force. In this Letter we will mainly address the issue of the driving mechanism.

Our experiments were carried out on 0.6–5 μm thick films of amorphous $\text{As}_2\text{S}_3(a\text{-As}_2\text{S}_3)$ glass prepared by thermal deposition (at 2×10^{-7} Torr) of bulk As_2S_3 on transparent microscope slides. The absorption coefficient of the obtained films was $\sim 10^3 \text{ cm}^{-1}$ at 514.5 nm. The RGs were formed using a standard holographic setup for spatially modulated excitation of ChG. The Ar^+ -ion laser (operating at 514.5 nm) beam was expanded to ensure a homogeneous polarization and/or intensity modulated exposure field over the whole examined region (diameter $\sim 1 \text{ cm}$). A beam splitter was used to obtain the two interfering beams. The angle between those beams could be adjusted providing spatial modulation periods between 4 and 30 μm . Polarizing Glan prisms and wave retarders (half wave or quarter wave plates) were used to obtain the desired intensity or polarization configuration. A He-Ne laser beam (operating at 632.8 nm) was used as a probe. The ChG samples were all photodarkened (i.e., exposed to circularly polarized laser beam at 514.5 nm) in order to completely saturate any photoinduced “scalar” effect. Note that the photodarkening does not affect the photoinduced vector effects due to the well-known fact that the scalar and vector effects are different at their origin [9]. The relief profiles were analyzed by means of both an atomic force microscope (AFM) and a DekTak profilometer. The preliminary scanning electron microscope analysis of the exposed region revealed no modulation of sulfur (S) and arsenic (As) concentrations, show-

ing that the RG formation process is compositionally uniform.

Experiments were carried out for both polarization modulation [resulting from the two right and left circularly polarized (hereafter RCP + LCP), two tilted linearly cross polarized (hereafter $45^\circ + 135^\circ$), or two s and p polarized (hereafter $s + p$) beams] and intensity modulation ($s + s$, $p + p$) configurations. We observed surface relief grating formation only in RCP + LCP or $45^\circ + 135^\circ$ configurations. Contrary to the experimental results presented in [6], in all the other configurations (including the $s + p$ orthogonal configuration) we did not detect any noticeable relief modulation. An AFM image of a typical RG with a period $\Lambda \approx 3.8 \mu\text{m}$, written on $5 \mu\text{m}$ thick chalcogenide film, is presented in the inset of Fig. 1. The grating was created in RCP + LCP configuration by exposing the film during 6 h 30 min at $I \approx 350 \text{ mW/cm}^2$ total excitation intensity (note that similar results were obtained for the $45^\circ + 135^\circ$ configuration, which are not shown here). The dependence of the peak-to-valley amplitude of the RG upon the exposure is presented in Fig. 1. After 36 h of excitation the modulation depth was measured to be $\sim 0.5 \mu\text{m}$, which corresponds to 10% of photoexpansion with respect to the film thickness. Still, the modulation amplitude keeps on increasing almost linearly with the exposure without apparently reaching any saturation even after 36 h. The relief modulation depends also on the period Λ of the polarization spatial modulation. This dependence has a nonmonotonic character (see Fig. 2), showing an optimum value for $\Lambda \approx 15 \mu\text{m}$. This value is surprisingly the same as that reported in [6], although the experimental conditions were different. The inscribed RGs were permanent, i.e., we could not erase them either by one beam exposure or by thermal annealing during 2 h keeping the film at $T \approx 178^\circ\text{C}$, which is near the glass transition temperature of $a\text{-As}_2\text{S}_3$ ($T_g \approx 180^\circ\text{C}$).

Since the RGs are obtained for configurations with no intensity modulation, the radiation pressure due to the light

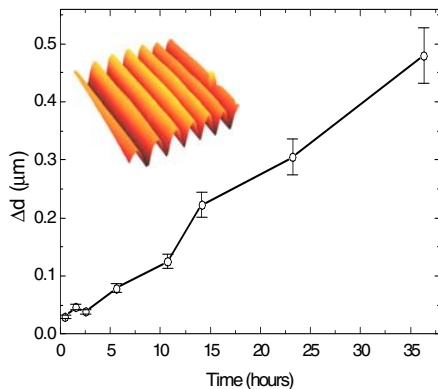


FIG. 1 (color online). Kinetics of RG formation on $5\text{-}\mu\text{m}$ -thick $a\text{-As}_2\text{S}_3$ chalcogenide film in RCP + LCP recording configuration: $\Lambda \sim 30 \mu\text{m}$, $I = 350 \text{ mW/cm}^2$; Δd is the relief modulation depth. In the inset is the AFM image of a typical RG recorded on the same film: $\Lambda \sim 3.8 \mu\text{m}$, $I = 350 \text{ mW/cm}^2$; $t_{\text{exp}} = 6 \text{ h } 30 \text{ min}$.

intensity gradient (see, e.g., [10]) is ruled out. Strictly speaking, small intensity modulations are still present in the (LCP + RCP) and ($45^\circ + 135^\circ$) orthogonal configurations, due to the nonzero crossing angle of recording beams. However, they do not play any role in the observed phenomenon in light of the absence of relief modulations in the ($s + s$) and ($p + p$) configurations, where the strongest intensity modulations are produced in the interference pattern. We believe rather that the internal forces giving rise to RG formation are related to the anisotropic volume changes reported in Ref. [11]. In that paper a linearly polarized near band gap illumination was shown to induce reversible volume changes (VCs) in similar chalcogenide glass. Accordingly, it was shown that a contraction was taking place in the direction parallel to the light polarization, whereas a dilatation was occurring in the perpendicular direction. In the case when exposing with a grating of polarization, one can thus speak about local contraction and dilatation, the direction of which being spatially modulated in the direction of the grating vector. Consequently, a periodically modulated volume stress will be produced. In the plane of the film surface the VCs perpendicular to the grating vector direction will be uniformly distributed over the whole surface of the glass resulting in no stress modulation, while the VCs in the direction of the grating vector will give rise to a periodic stress modulation. Let us consider in more detail the mechanism of generation of internal gradient force, which would initiate such a mass transport.

According to the phenomenological model of photo-induced anisotropy proposed by Fritzsche [12] for chalcogenide glasses, the isotropy that is observed at the macroscopic level actually results from the averaging of an ensemble of anisotropic microvolumes (AMVs) corresponding to polarizable anisotropic units (native or photo-induced). The light illumination excites preferentially the AMVs oriented so that they present the highest absorption cross section in the direction of its polarization. As a

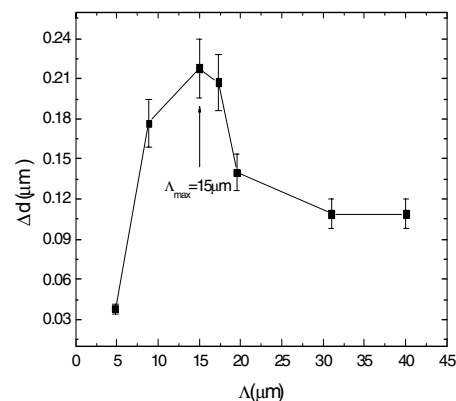


FIG. 2. Dependence of the relief modulation depth (Δd) on the grating period in $5\text{-}\mu\text{m}$ -thick $a\text{-As}_2\text{S}_3$ chalcogenide film; RCP + LCP recording configuration; $I = 350 \text{ mW/cm}^2$, $t_{\text{exp}} = 6 \text{ h } 30 \text{ min}$.

consequence, the AMVs are redistributed in such a way as to minimize the absorption in light polarization direction, giving rise to a macroscopic anisotropy. Following this approach and according to the results reported in [13], we postulate for the existence of uniaxial ellipsoidal microvolumes, which reorient themselves under the action of light exposure. The macroscopic volume contribution of these AMVs in the x dimension (direction of the grating vector) depends on the angular distribution of the axes of symmetry of these AMVs. This angular distribution, resulting from the photoexposure, in its turn depends strongly upon the form of the linear polarizability tensor β_{ij} of the AMVs. One can distinguish two phenomenological models of these AMVs: cigarlike, when $\beta_{\parallel} > \beta_{\perp}$ and $r_{\parallel} > r_{\perp}$, and disklike, when $\beta_{\parallel} < \beta_{\perp}$ and $r_{\parallel} < r_{\perp}$, the β_{\parallel} , β_{\perp} and r_{\parallel} , r_{\perp} being the polarizabilities and radii parallel and perpendicular to the axis of symmetry of the ellipsoid of revolution, respectively. Recently we showed the disklike model of the linear polarizability tensor of AMVs to be more appropriate for the description of photo-induced anisotropy in a -As₂S₃ chalcogenide glass [13]. In the following we shall still consider both models of the AMVs for comparison. For a given angular distribution of the axes of AMVs, the macroscopic contribution of these AMVs to the length of the infinitely small segment δx , for a small anisotropy approximation, will be (which is valid for both models)

$$\Delta_x = \left\{ N_0 r_{\perp} + (r_{\parallel} - r_{\perp}) \int_{4\pi} N(\theta, \varphi) n_x^2 d\Omega \right\} \delta x, \quad (1)$$

where $N(\theta, \varphi)$ is the number of AMVs oriented, per unit solid angle per unit segment (in the x direction), $N_0 = \int_{4\pi} N(\theta, \varphi) d\Omega$ is the total number of AMVs per unit segment, φ and θ are spherical polar coordinates, $d\Omega = \sin\theta d\theta d\varphi$ is an element of solid angle, and $n_x = \sin\theta \cos\varphi$ is the x projection of the unit vector \mathbf{n} which is aligned in the direction of the axis of symmetry of the AMV.

For simplicity we consider an idealized situation in which all AMVs are in their excited photostationary state. Let us first discuss the disklike model and make some simplifying assumptions to construct the $N(\theta, \varphi)$ function; i.e., we assume, as in [13], that the axes of symmetry of AMVs will tend to get completely oriented in the direction of the electric field in the case of linear polarization of excitation and uniformly distributed in the plane perpendicular to the light propagation direction in the case of circular polarization. Next, assuming a linear dependence of $N(\theta, \varphi, e)$ on the polarization ellipticity, one has

$$N(\theta, \varphi, e) = (N_0 / \sin\theta) \delta(\theta - \pi/2) \times [e(x)/2\pi + (1 - e(x))\delta(\varphi - \varphi_0(x))], \quad (2)$$

where $0 \leq e(x) \leq 1$ is the spatially varying polarization ellipticity of the excitation, $\varphi_0(x)$ is the angle between the long axis of the ellipse of polarization and the x direction, and δ is the Dirac delta function. From Eqs. (1) and (2) the

relative (dimensionless) VC in the x direction will be

$$X_R(x) \equiv \Delta_x / \delta x = N_0 \{ r_{\perp} + (r_{\parallel} - r_{\perp}) \times [e(x)/2 + (1 - e(x))\cos^2\varphi_0(x)] \}. \quad (3)$$

Taking as a reference the VC corresponding to circular polarization (the polarization of excitation that is used to saturate the scalar effects in the sample prior to vectorial grating recording), the relative VC in the x direction will be

$$\Delta X_R(x) \equiv X_R - X_R^c = N_0(1 - e(x))(r_{\parallel} - r_{\perp})[\cos^2\varphi_0(x) - 1/2], \quad (4)$$

where $X_R^c = N_0(r_{\parallel} + r_{\perp})/2$ corresponds to a circularly polarized excitation. Equation (4) is accounting for our experimental results. Indeed, in the LCP + RCP case, when $e(x) = 0$ and $\varphi_0(x) = \pi x/\Lambda$, one has

$$\Delta X_R(x) = N_0(r_{\parallel} - r_{\perp})[\cos^2(\pi x/\Lambda) - 1/2]. \quad (5)$$

According to Eq. (5), in the regions where the interference pattern results in linear horizontal light polarization (recalling that the sample film is vertical and the excitation grating vector is in that plane, in the horizontal direction), ΔX_R is negative and a contraction occurs parallel to the direction of the grating vector contrary to regions exposed with vertical polarization, where dilatation will take place in this direction [see Fig. 3(a)]. The contraction/dilatation function in the $45^\circ + 135^\circ$ case is presented in Fig. 3(b).

From Eq. (4) it follows that $\Delta X_R = 0$ in the $s + p$ configuration since $\varphi_0 = \pm\pi/4$, and hence there are no spatially modulated VCs. Thus the disklike model predicts uniform VCs over the whole film surface in this excitation configuration resulting in no relief modulation, in agreement with our experimental results. Note that the presence

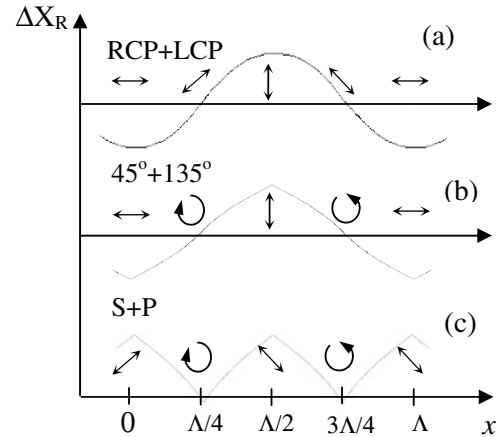


FIG. 3. The resultant polarization state of the interference grating and corresponding contraction/dilatation function (ΔX_R) for (a) RCP + LCP and (b) $45^\circ + 135^\circ$ excitation configurations for the disklike model and (c) $s + p$ configuration for the cigarlike model. The peaks of the RGs correspond to the maximums of the local contraction.

of relief modulations in the $s + p$ case (reported in [6]) is rather difficult to analyze due to the high intensities, non-ideal orthogonality of the exposure configuration, and the use of nonphotodarkened samples that could contribute to give rise to relief modulations.

In contrast to the disklike model, the cigarlike model predicts two key phenomena that are not observed experimentally in the $s + p$ excitation configuration. Indeed, one can derive the corresponding expression for this model:

$$\Delta X_R \equiv X_R - X_R^c = (N_0/2)(r_{\parallel} - r_{\perp})(1 - e(x))\sin^2\varphi_0(x), \quad (6)$$

where $X_R^c = N_0 r_{\perp}$. Equation (6) predicts periodic VCs in the $s + p$ case ($\varphi_0 = \pm\pi/4$) due to the periodically varying ellipticity $e(x)$ and hence a relief modulation, which has two times smaller period as compared to that of the RCP + LCP case. The peaks of the relief grating will correspond to circular polarization in the polarization pattern, where maximum contraction takes place [see Fig. 3(c)]. This kind of phenomenon has already been observed experimentally in liquid crystalline azobenzene side-chain polyester, where cigarlike anisotropic units are at the origin of relief modulation [14]. However, in our material, we were not able to observe RG formation in either the $s + p$ case or double frequency modulation.

We believe that the effect of the photoexcitation is not limited to the creation of periodic stress in the ChG film. The second important effect of spatially uniform photoexcitation is the photoinduced softening of the ChG matrix that concurs to significantly decrease the viscosity of the medium and, consequently, facilitate the film deformation. This softening (otherwise called photoinduced electronic fluidity) is not a thermal process (which we have verified experimentally) but rather a result of the photoinduced intermolecular bond breaking or weakening (see, e.g., [3,15]). The long (tens of hours) characteristic time of RG formation is also in favor of the model of the mass transport, since the stress formation is a much faster process (several minutes, see [11]). We also believe that the existence of an optimal grating period ($\Lambda \approx 15 \mu\text{m}$, see Fig. 3) is a result of two opposing forces, similar to the situation described in Ref. [6]. Namely, one of these forces is the driving internal gradient force, which, as follows from Eq. (5), is inversely proportional to the grating period, $F_{\text{int}} \sim d(\Delta X_R)/dx \sim \Lambda^{-1}$. The other force is the surface tension, which acts in the opposite direction and is proportional to Λ^{-2} . This intriguing phenomenon is currently under study and will be discussed in more detail soon.

We tried also to record the RG in $45^\circ + 135^\circ$ writing configuration using sub-band-gap and nonresonant red light illumination from a He-Ne laser operating at 632.8 nm. The recording beams were focused to ensure the same recording intensities as in the case of green light recording. No relief modulation was observed even when adding a simultaneous excitation with uniform (both intensity and polarization) beam at 514.5 nm, in order to simultaneously

decrease the viscosity. This further supports our model assuming that, unlike the green resonant illumination, the low intensity red light cannot initiate the AMV realignment process, and hence the spatially varying stress in the glass which is at the origin of the mass transport.

As for microscopic interpretation of AMVs, it is important to note that a similar link between the photoanisotropic and the contraction/dilatation properties of ChGs was previously established in Ref. [11], where a realistic microscopic interpretation was given of the uniform contraction/dilatation in the As-Se glass thin film. This interpretation, which was based on As-Se-AS triangle units as basic anisotropic units, is perfectly consistent with our disklike shape model.

In conclusion, we have reported on giant relief modulations created in chalcogenide $a\text{-As}_2\text{S}_3$ glass by exposing it to intensity uniform but polarization modulated resonant (band gap) light illumination. A mechanism based on spatially periodic contraction/dilatation is proposed to successfully explain the observed phenomena. As a result, volume stress modulation and consequently mass transport in the direction of this modulation are generated, giving rise to a strong relief modulation. The validity of the disklike phenomenological model of the AMVs was also demonstrated.

We would like to thank the Canadian Institute for Photonic Innovations for financial support and Victor Tikhomirov for useful discussions.

*Also at: Photointech, Inc., 2740 Einstein, Sainte-Foy, Quebec, Canada G1P4S4.

- [1] *Handbook of Advanced Electronic and Photonic Materials and Devices*, edited by H. S. Nalwa (Academic, San Diego, 2001), Vol. 5.
- [2] J. Gump *et al.*, Phys. Rev. Lett. **92**, 245501 (2004).
- [3] T. Galstian, J.-F. Viens, A. Villeneuve, K. Richardson, and M. A. Duguay, Lightwave Technology **15**, 1343 (1997).
- [4] S. Ramachandran, S. G. Bishop, J. P. Guo, and D. J. Brady, IEEE Photonics Technol. Lett. **8**, 1041 (1996).
- [5] S. H. Messaddeq, V. K. Tikhomirov, Y. Messaddeq, D. Lezal, and M. S. Li, Phys. Rev. B **63**, 224203 (2001).
- [6] A. Saliminia, T. V. Galstian, and A. Villeneuve, Phys. Rev. Lett. **85**, 4112 (2000).
- [7] K. E. Asatryan, S. Fr  d  rick, T. Galstian, and R. Vall  e, Appl. Phys. Lett. **84**, 1626 (2004).
- [8] L. Nikolova and T. Todorov, Opt. Acta **31**, 579 (1984).
- [9] V. M. Lyubin and V. K. Tikhomirov, J. Non-Cryst. Solids **114**, 133 (1989).
- [10] J. M. Gordon, Phys. Rev. A **8**, 14 (1973).
- [11] P. Krecmer, A. M. Moulin, R. J. Stephenson, T. Rayment, M. E. Welland, and S. R. Elliot, Science **277**, 1799 (1997).
- [12] H. Fritzsche, Phys. Rev. B **52**, 15 854 (1995).
- [13] K. E. Asatryan, B. Paquet, T. V. Galstian, and R. Vall  e, Phys. Rev. B **67**, 014208 (2003).
- [14] T. G. Pedersen, P. M. Johansen, N. C. R. Holme, P. S. Ramamujam, and S. Hvilsted, Phys. Rev. Lett. **80**, 89 (1998).
- [15] H. Hisakuni and K. Tanaka, Science **270**, 974 (1995).